Supporting Information

D. Coumou et al., "Quasi-resonant circulation regimes and hemispheric synchronization of extreme weather in boreal summer"

Methods

We use daily wind field data from ERA Interim reanalysis (41) for the months of July and August over the period 1979-2012. For each individual day, we determine the amplitude and phase for each wave number by taking a Fast Fourier Transform (FFT) of the meridional wind at 500mb averaged from 35°N to 65°N. We calculate the phase speed (eastward propagation) of each wave by taking a fourth-order accurate numerical approximation of the transient derivative of its phase. We tried different numerical methods to calculate the derivative and found the estimate of the phase speed to be robust. We also found the results to be insensitive to the exact choice of latitudinal boundaries. The 2D probability density functions (Fig. 2 and 3) are obtained by applying a non-parametric kernel density estimation to the daily spectral data. The power density field (Fig. 2d) is obtained by multiplying the frequency-density of a wave number and phase speed combination with the square of the mean amplitude of that particular wave number and phase speed combination. Zonal-mean zonal wind (Fig. 3) is determined over the same latitudinal belt, i.e.,35°N to 65°N.

To quantify the hemispheric-wide occurrence of extremes, we define the mid-latitude extreme (MEX) index:

$$MEX(x,t) = \left(\frac{1}{N} \sum_{i}^{N} \left(\frac{\Delta x_i(t)}{\sigma(x_i)} \right)^2 - \mu_{MEX} \right) \Big/ \sigma_{MEX}$$

Here x refers to any meteorological variable defined on a mid-latitudinal grid consisting of N individual grid-points at timestep t. The MEX index is calculated for each calendar day or calendar month separately, creating single values for each year. We first use a singular spectrum analysis to extract the long-term non-linear trend of x. The anomaly $\Delta x_i(t)$ is the deviation of x from this long-term non-linear trend at grid point i. By detrending the data, we prevent that long-term trends (i.e.,warming) contribute to an increase in the index, since we are only interested in how specific circulation regimes affect surface extremes. $\sigma(x_i)$ is the standard deviation of the detrended data. The MEX index is normalized by

subtracting its time-averaged value (μ_{MEX}) and dividing by its standard deviation (σ_{MEX}), making it a dimensionless quantity with a time-mean value of 0. We determined MEX for the hemispheric-band stretching from 35°N to 65°N (as in the Fourier Analysis) and for positive extremes in temperature (heat-extremes) and precipitation (heavy rainfall) using monthly and daily data from the ERA Interim reanalysis (41).

TABLE 1 - Cluster Analysis

	Era Interim (500mb)		**Era Interim (300mb)**		**NCEP-NCAR (500mb)**		**NCEP-NCAR (300mb)**	
	KS-test	MW-test	KS-test	MW-test	KS-test	MW-test	KS-test	MW-test
quasi-stationary (|c| < 2m/s)	Figure 6		Figure S1		Figure S2		Figure S3	
wave 6	0.38	0.30	0.70	0.74	0.55	0.60	0.43	0.64
wave 7	0.05	0.01	0.06	0.02	0.01	0.01	0.01	0.01
wave 8	0.48	0.34	0.07	0.34	0.06	0.02	0.30	0.21
quasi-stationary (|c| < 2m/s)	Figure S4		Figure S5		Figure S6		Figure S7	
wave 6+7+8	0.28	0.24	0.01	0.04	0.28	0.28	0.01	0.01
wave 6+7	0.54	0.43	0.13	0.07	0.54	0.54	0.03	0.01
wave 7+8	0.04	0.01	0.01	0.03	0.04	0.04	0.01	0.01
transient (c > 4m/s)	Figure S8		Figure S9		Figure S10		Figure S11	
wave 6	0.42	0.15	0.24	0.36	0.20	0.21	0.67	0.86
wave 7	0.86	0.86	0.84	0.75	0.67	0.41	0.68	0.81
wave 8	0.50	0.41	0.72	0.35	0.16	0.14	0.56	0.64
wave 6+7+8	0.15	0.19	0.34	0.20	0.59	0.29	0.44	0.56
wave 6+7	0.42	0.30	0.31	0.37	0.82	0.87	0.54	0.76
wave 7+8	0.36	0.47	0.58	0.37	0.80	0.60	0.39	0.60

Table S1: Statistical significance of changes in the amplitude distribution of quasi-stationary (|c| < 2m/s) and transient (c > 4m/s) planetary waves for 2000-2012 compared to 1979-1999. For each individual wave number (6-8) and combinations of them, the p-value is calculated using a Kolmogorov-Smirnov (KS) test and a Mann-Whitney (MW) test. The observed shift in the distribution towards higher amplitudes for quasi-stationary waves with wave number 7 (Figure 6) and the combination of wave numbers 7 and 8 (Figure S1-S7) is statistically significant at 95% confidence (p-values printed in red) for both reanalysis products and both pressure levels. None of the changes in the amplitude distribution of transient waves are statistically significant.

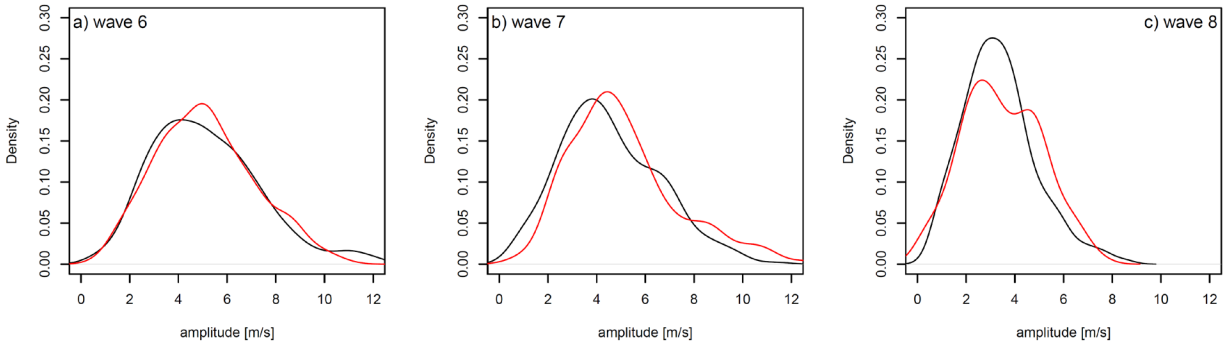

Fig. S1: Probability density distributions of amplitudes of quasi-stationary waves ($|c| < 2$ m/s) at 300mb for days in July-August during 1979-1999 (black) and 2000-2012 (red) for (a) wave 6, (b) wave 7 and (c) wave 8 in the Era Interim reanalysis. The shift in the distribution of wave 7 to higher amplitudes is statistically significant at 95% confidence (see Table S1).

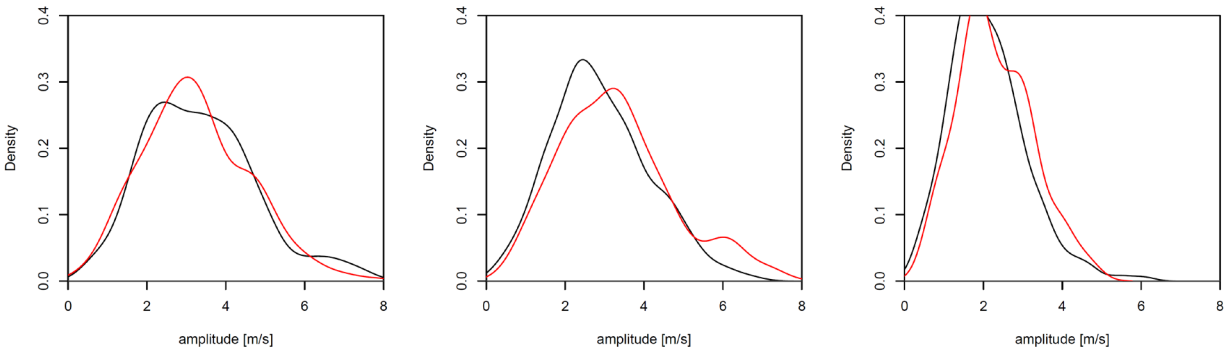

Fig. S2: Probability density distributions of amplitudes of quasi-stationary waves ($|c| < 2$ m/s) at 500mb for days in July-August during 1979-1999 (black) and 2000-2012 (red) for (a) wave 6, (b) wave 7 and (c) wave 8 in the NCEP-NCAR reanalysis. The shift in the distribution of wave 7 to higher amplitudes is statistically significant at 95% confidence (see Table S1).

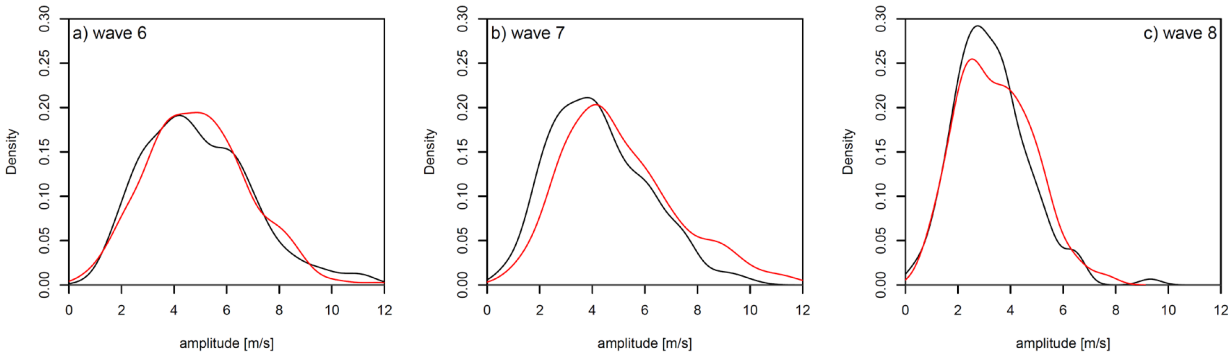

Fig. S3: Probability density distributions of amplitudes of quasi-stationary waves ($|c| < 2$ m/s) at 300mb for days in July-August during 1979-1999 (black) and 2000-2012 (red) for (a) wave 6, (b) wave 7 and (c) wave 8 in the NCEP-NCAR reanalysis. The shift in the distribution of wave 7 to higher amplitudes is statistically significant at 95% confidence (see Table S1).

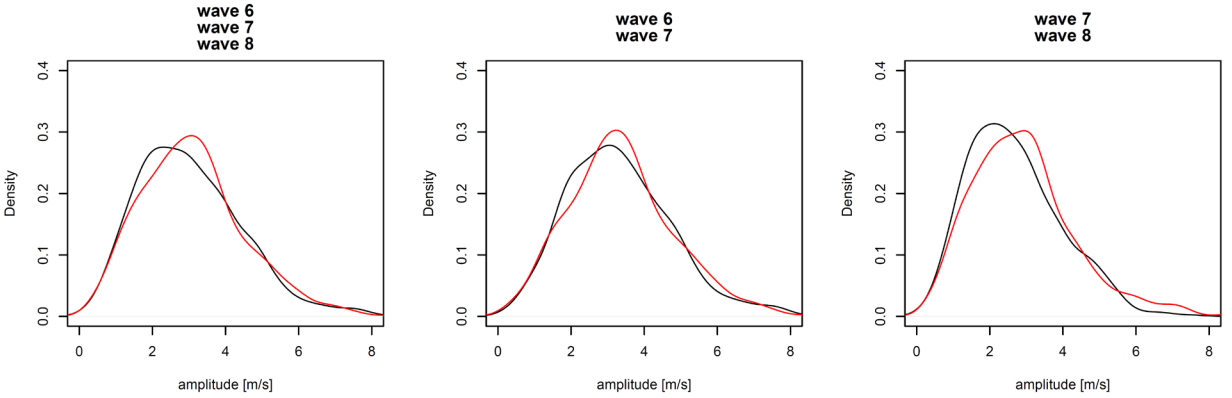

Fig. S4: Probability density distributions of amplitudes of quasi-stationary waves ($|c| < 2$ m/s) at 500mb for days in July-August during 1979-1999 (black) and 2000-2012 (red) for (a) waves 6, 7 and 8, (b) wave 6 and 7 and (c) wave 7 and 8 in the Era Interim reanalysis. The shift in the combined distribution of waves 7 and 8 (right panel) is statistically significant at 95% confidence (see Table S1).

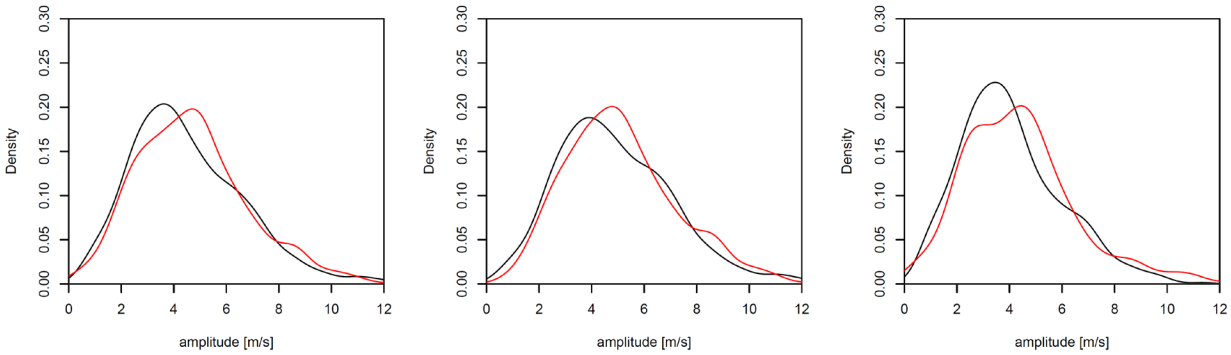

Fig. S5: Probability density distributions of amplitudes of quasi-stationary waves ($|c| < 2$ m/s) at 300mb for days in July-August during 1979-1999 (black) and 2000-2012 (red) for (a) waves 6, 7 and 8, (b) wave 6 and 7 and (c) wave 7 and 8 in the Era Interim reanalysis. The shift in the combined distribution of waves 6, 7 and 8 (left panel) and 7 and 8 (right panel) is statistically significant at 95% confidence (see Table S1).

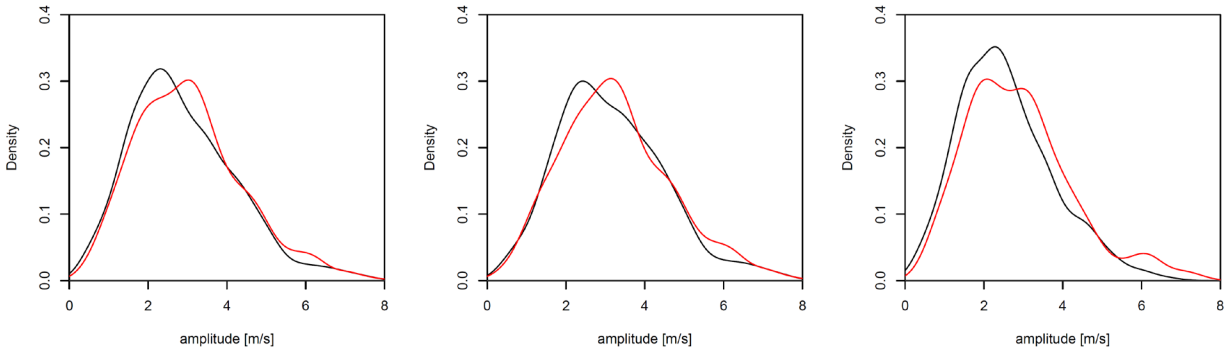

Fig. S6: Probability density distributions of amplitudes of quasi-stationary waves ($|c| < 2$ m/s) at 500mb for days in July-August during 1979-1999 (black) and 2000-2012 (red) for (a) waves 6, 7 and 8, (b) wave 6 and 7 and (c) wave 7 and 8 in the NCEP-NCAR reanalysis. The shift in the combined distribution of waves 7 and 8 (right panel) is statistically significant at 95% confidence (see Table S1).

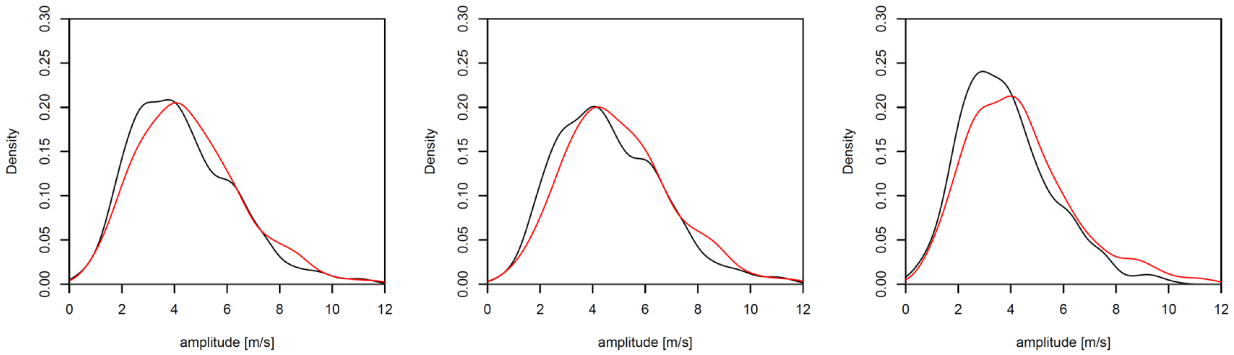

Fig. S7: Probability density distributions of amplitudes of quasi-stationary waves ($|c| < 2$ m/s) at 300mb for days in July-August during 1979-1999 (black) and 2000-2012 (red) for (a) waves 6, 7 and 8, (b) wave 6 and 7 and (c) wave 7 and 8 in the NCEP-NCAR reanalysis. All shifts in these distributions are statistically significant at 95% confidence (see Table S1).

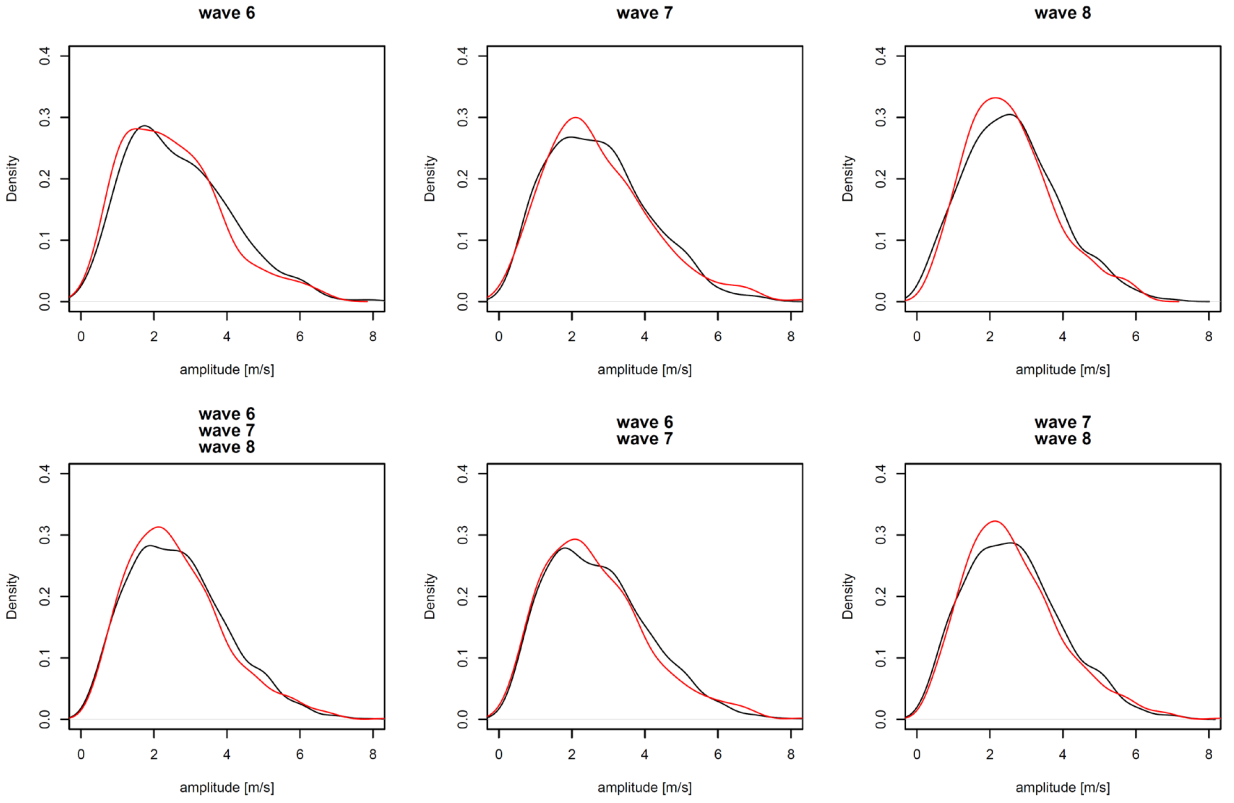

Fig. S8: Probability density distributions of amplitudes of transient waves ($c > 4$ m/s) at 500mb for days in July-August during 1979-1999 (black) and 2000-2012 (red) for (a) waves 6, (b) wave 7, (c) wave 8, (d)

waves 6, 7 and 8, (e) wave 6 and 7 and (f) wave 7 and 8 in the Era Interim reanalysis. None of the changes in distributions are statistically significant (see Table S1).

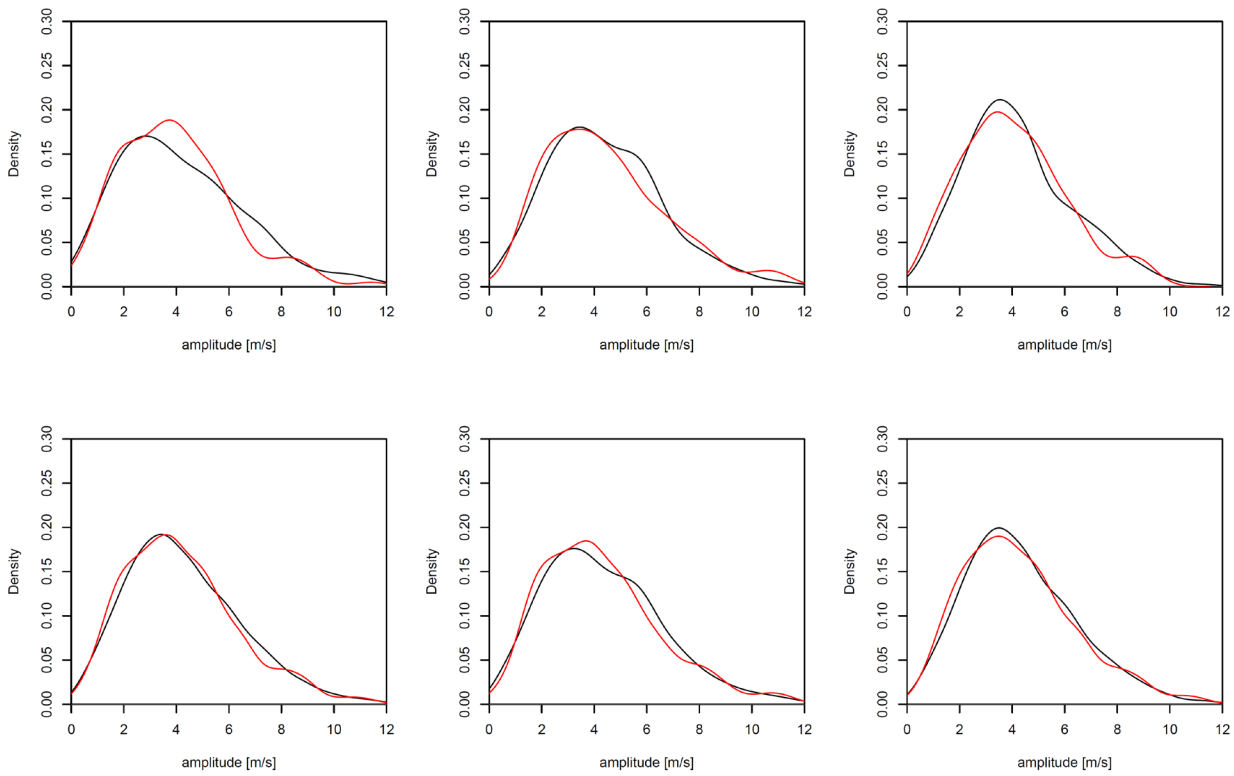

Fig. S9: Probability density distributions of amplitudes of transient waves (c > 4 m/s) at 300mb for days in July-August during 1979-1999 (black) and 2000-2012 (red) for (a) waves 6, (b) wave 7, (c) wave 8, (d) waves 6, 7 and 8, (e) wave 6 and 7 and (f) wave 7 and 8 in the Era Interim reanalysis. None of the changes in distributions are statistically significant (see Table S1).

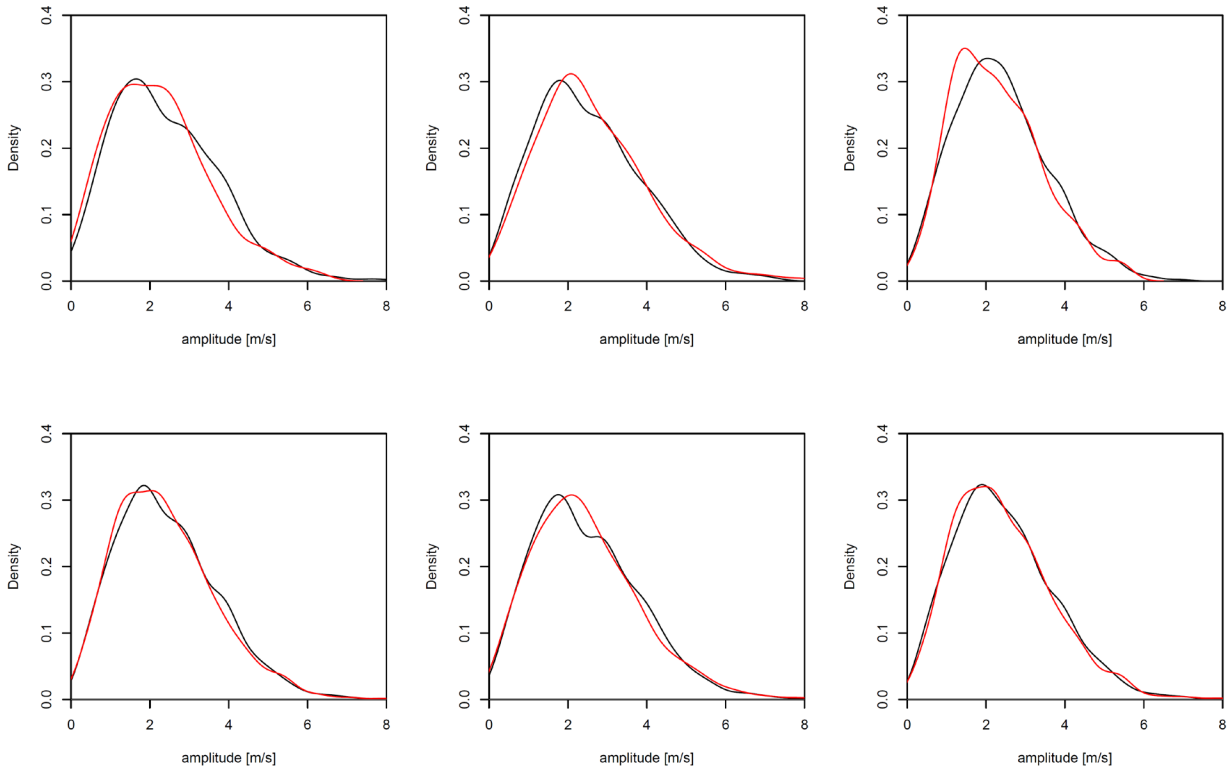

Fig. S10: Probability density distributions of amplitudes of transient waves (c > 4 m/s) at 500mb for days in July-August during 1979-1999 (black) and 2000-2012 (red) for (a) waves 6, (b) wave 7, (c) wave 8, (d) waves 6, 7 and 8, (e) wave 6 and 7 and (f) wave 7 and 8 in the NCEP-NCAR reanalysis. None of the changes in distributions are statistically significant (see Table S1).

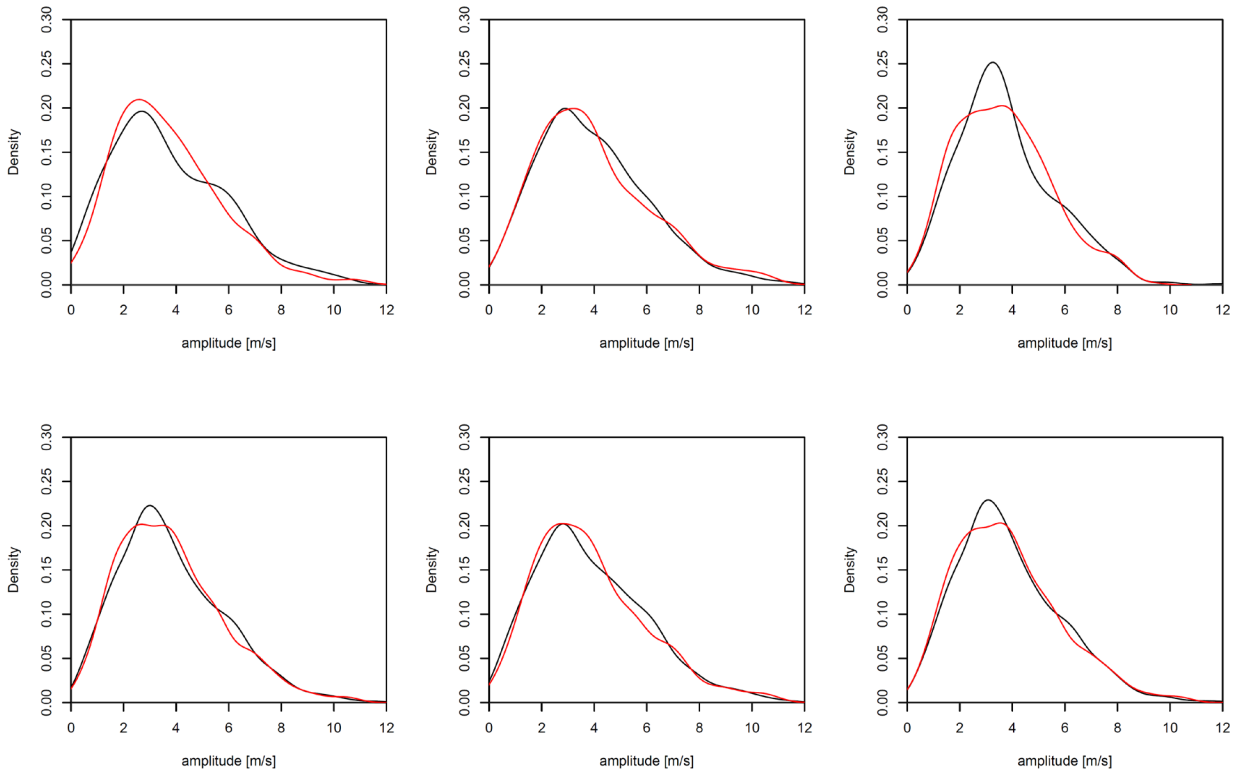

Fig. S11: Probability density distributions of amplitudes of transient waves ($c > 4$ m/s) at 300mb for days in July-August during 1979-1999 (black) and 2000-2012 (red) for (a) waves 6, (b) wave 7, (c) wave 8, (d) waves 6, 7 and 8, (e) wave 6 and 7 and (f) wave 7 and 8 in the NCEP-NCAR reanalysis. None of the changes in distributions are statistically significant (see Table S1).

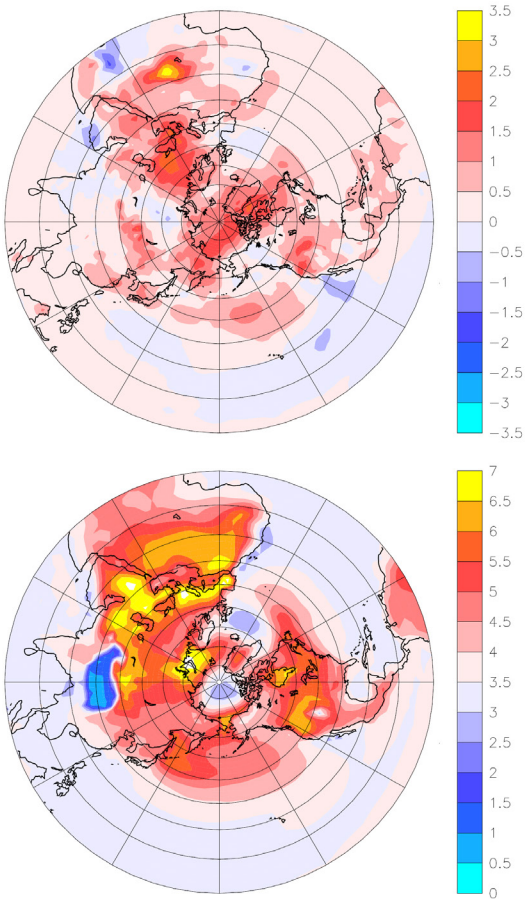

Fig. S12: Stereographic polar projections of July-August temperature anomaly at 1000mb for (top) 2000-2012 compared to 1979-1999 of the Era-interim reanalysis, and for (bottom) 2081-2100 compared to 1981-2000 of the multi-model mean of the CMIP5 set of climate projections under scenario RCP8.5.